Imaging Science in Dentistry 2023; 53: 375-81
https://doi.org/10.5624/isd.20230157

Diagnostic performance of stitched and non-stitched cross-sectional cone-beam computed tomography images of a non-displaced fracture of ovine mandibular bone

Farzane Ostovarrad[1], Sadra Masali Markiyeh[1], Zahra Dalili Kajan[1,2,*]

[1]*Department of Maxillofacial Radiology, School of Dentistry, Guilan University of Medical Sciences, Rasht, Iran*
[2]*Dental Sciences Research Center, School of Dentistry, Guilan University of Medical Sciences, Rasht, Iran*

ABSTRACT

Purpose: This study assessed the diagnostic performance of stitched and non-stitched cross-sectional cone-beam computed tomography (CBCT) images of non-displaced ovine mandibular fractures.

Materials and Methods: In this *ex vivo* study, non-displaced fractures were artificially created in 10 ovine mandibles (20 hemi-mandibles) using a hammer. The control group comprised 8 hemi-mandibles. The non-displaced fracture lines were oblique or vertical, <0.5 mm wide, 10-20 mm long, and only in the buccal or lingual cortex. Fracture lines in the ramus and posterior mandible were created to be at the interface or borders of the 2 stitched images. CBCT images were obtained from the specimens with an 80 mm $\times$ 80 mm field of view before and after fracture induction. OnDemand software (Cybermed, Seoul, Korea) was used for stitching the CBCT images. Four observers evaluated 56 (28 stitched and 28 non-stitched) images to detect fracture lines. The diagnostic performance of stitched and non-stitched images was assessed by calculating the area under the receiver operating characteristic curve (AUC). Sensitivity and specificity values were also calculated (alpha $=0.05$).

Results: The AUC was calculated to be 0.862 and 0.825 for the stitched and non-stitched images, respectively ($P=0.747$). The sensitivity and specificity were 90% and 75% for the non-stitched images and 85% and 87% for the stitched images, respectively. The inter-observer reliability was shown by a Fleiss kappa coefficient of 0.79, indicating good agreement.

Conclusion: No significant difference was found in the diagnostic performance of stitched and non-stitched cross-sectional CBCT images of non-displaced fractures of the ovine mandible. ***(Imaging Sci Dent 2023; 53: 375-81)***

KEY WORDS: Cone-Beam Computed Tomography; Fractures, Bone; Mandible; Imaging, Three dimensional

Introduction

Cone-beam computed tomography (CBCT) is essential in diagnosis, treatment planning, and the assessment of treatment outcomes.[1-5] Such a wide range of applications requires various sizes of field of view (FOV) and voxel size (resolution).[6] FOV dimensions depend on the detector size, beam geometry, and beam collimation. Since the detector accounts for a large proportion of the fabrication cost of CBCT scanners, an efficient approach is required to scan a larger area without requiring a larger detector.[7,8] CBCT scanners are classified according to their maximum size of FOV, composed of 1 or more scans.

One suggested strategy to scan a region of interest (ROI) larger than the detector FOV is to collect data from 2 or more individual scans and superimpose and overlap the volumetric CBCT data by using reliable reference landmarks. This process is known as bioimage registration or mosaicking. Software programs can be used to stitch or blend adjacent volumetric images and compile larger volumes of data in horizontal or vertical dimensions. Stitching can be performed both vertically (to increase height) and horizontally (to increase width).[7]

According to Kopp and Ottl,[9] surgeons often prefer to use

Received July 19, 2023; Revised September 26, 2023; Accepted October 11, 2023
Published online November 6, 2023
*Correspondence to : Prof. Zahra Dalili Kajan
Department of Dentomaxillofacial Radiology, Dental Sciences Research Center, Guilan University of Medical Sciences, End of Professor Samii Blvd, 41941-73774, Rasht, Iran
Tel) 98-911-1343432, E-mail) zahradalili@yahoo.com

CBCT scanners with a large FOV, while general dentists are more interested in multipurpose systems with higher resolution; however, such systems cannot image both jaws due to their small FOV. This limitation becomes particularly problematic in the fields of maxillofacial surgery and implant placement. A potential solution to this issue is to stitch or fuse 2 or more smaller volumes to create a larger volume.

Stitching can be performed either manually, using third-party software, or automatically with a specific CBCT software program.[1,5] Stitching enables the evaluation of a larger volume with optimal resolution. However, it still has limitations, such as longer scanning time, higher risk of motion artifacts, double exposure, and overlapping of scanned areas.[1,6,7,9] Although automatic stitching is independent of the operator, patient movement during exposures can affect the results. This means that the production of a composite image does not necessarily ensure dimensional stability, due to potential motion artifacts between exposures.

A noteworthy issue is that successful treatment requires accurate information obtained from 2-dimensional and 3-dimensional images, especially for linear measurements. Therefore, a previous study evaluated the accuracy of linear measurements made on stitched CBCT images, and the results showed that linear measurements were accurate and reliable.[9] Moreover, evidence shows that the object position affects the diagnostic accuracy; specifically, the diagnostic accuracy at the center of the FOV is higher than that in peripheral areas.[10] This issue may also affect stitched images. According to the literature, the accuracy of CBCT for detecting bone fractures may change the treatment plan in some cases. Moreover, aside from treatment planning, CBCT plays a critical role in detecting the cause of pain in many patients.[11,12]

Considering the extensive applications of CBCT in maxillofacial assessments and the detection of bone fractures, such as non-displaced fractures (i.e., linear fractures in which the proximal segment maintains its normal anatomical relation to the distal segment),[13] and the existing information gap regarding the diagnostic performance of stitched images for detecting non-displaced mandibular fractures, this study investigated the diagnostic performance of stitched and non-stitched cross-sectional CBCT images of non-displaced ovine mandibular fractures.

Materials and Methods

The protocol of this *ex vivo* experimental study was approved by the ethics committee of Guilan University of Medical Sciences (IR.GUMS.REC.1401.424).

The minimum sample size was calculated to be 28 in each group according to a previous study,[14] assuming alpha = 0.05, 90% study power, and the area under the receiver operating characteristic curve (AUC) to be 0.567 for stitched and 0.833 for full-FOV images using MedCalc version 20.026 software.

Non-displaced oblique or vertical fractures were artificially created in the right and left quadrants of 10 ovine mandibles (20 hemi-mandibles as an experimental group) using a hammer. The mandibles crushed by the hammer impact were excluded and replaced by others. The remaining 8 hemi-mandibles were used as the control group and remained sound with no fracture.

The non-displaced fracture lines were horizontal, had a width of <0.5 mm and a length of 10-20 mm, and were only in the buccal or lingual cortex (Fig. 1). Fracture lines in the ramus and posterior mandible were created such that they were located at the interface or borders of the 2 stitched images. A CBCT scanner (Vatech, Hwaseong, Korea) was used to image the mandibles. The exposure settings were adjusted to an 80×80 mm FOV, a 0.2-mm standard voxel size, 5.2 mA, and 95 kVp. The CBCT images were taken in 2 sets, before and after stitching the images. All mandibles were coated with 2 layers of 2-mm-thick dental wax[15] for soft tissue simulation. The FOV and exposure

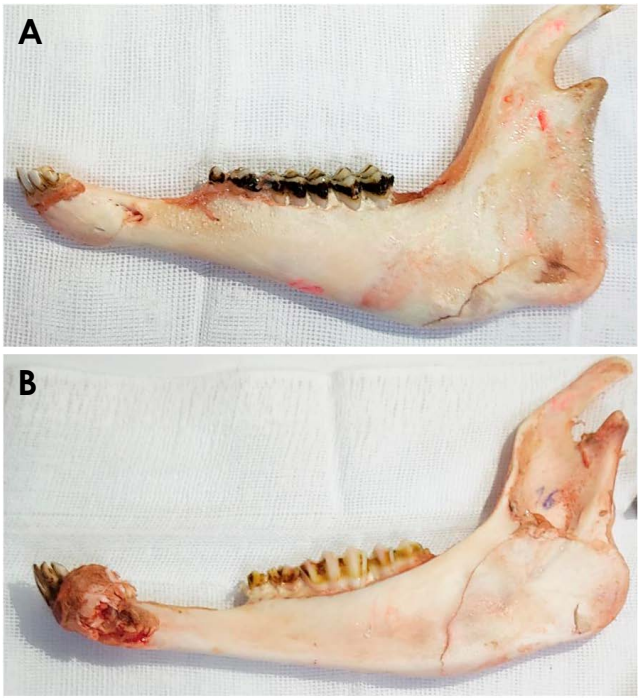

Fig. 1. An artificial fracture induced on the buccal (A) and lingual (B) aspects of the ovine semi-mandibles.

Fig. 2. Superimposition of 2 parts of the mandible in axial, sagittal, and 3-dimensional sections using OnDemand software to stitch the cone-beam computed tomographic images.

parameters were the same in both scan series to eliminate the effect of confounders (FOV and exposure settings) on image reconstruction.

In the non-stitched series, the entire length of mandibles was imaged in an 80 × 80 mm FOV. In the second series, 2 scans were obtained from each mandible to create stitched images. The first scan of the stitched image included the condyle to half the distance between the crest and the inferior border of the mandible. The second scan included the bone crest to the inferior border of the mandible. The images were stitched using OnDemand software (Cybermed, Seoul, Korea). For stitching the images, 3 points in the mandible were superimposed, including (1) the mandibular crest adjacent to the distal surface of the last tooth, (2) the mandibular crest adjacent to the mesial surface of the first series of posterior teeth, and (3) the most posterior part of the posterior ramus border (Fig. 2). Then, cross-sectional views with a 1 mm slice thickness and 1 mm slice interval were reconstructed. Next, the selected cross-sectional views were extracted for assessment by the observers (Fig. 3). Notably, the same methods were chosen for the reconstruction and selection of the cross-sectional views from non-stitched images. Figure 4 shows 2 series of non-stitched and stitched cross-sectional images of the ovine mandible with fracture.

Subsequently, 4 observers with 6-8 years of experience in their specialties, including 2 assistant professors of oral radiology and 2 assistant professors of oral and maxillofacial surgery for detecting fracture lines. The observations were done under standard lighting conditions on a 21-inch monitor (LG, Seoul, Korea). The CBCT scans were assessed again by the same observers after a 4-week interval to calculate intra-observer reliability.

The Fleiss kappa coefficient of agreement was calculated to assess intra-observer and inter-observer reliability. The diagnostic performance of the stitched and non-stitched images was assessed by calculating the AUC. Sensitivity and specificity values were also calculated. The method of DeLong et al. was used to calculate the standard error. The binomial exact method was used to calculate the confidence interval for the AUC, and the method of DeLong et al.[16] was applied to compare the stitched and full-FOV images. Data were analyzed using SPSS version 28 (IBM Corp., Armonk, NY, USA) and MedCalc version 20.026 (MedCalc Software Ltd., Ostend, Belgium) at a 0.05 significance level.

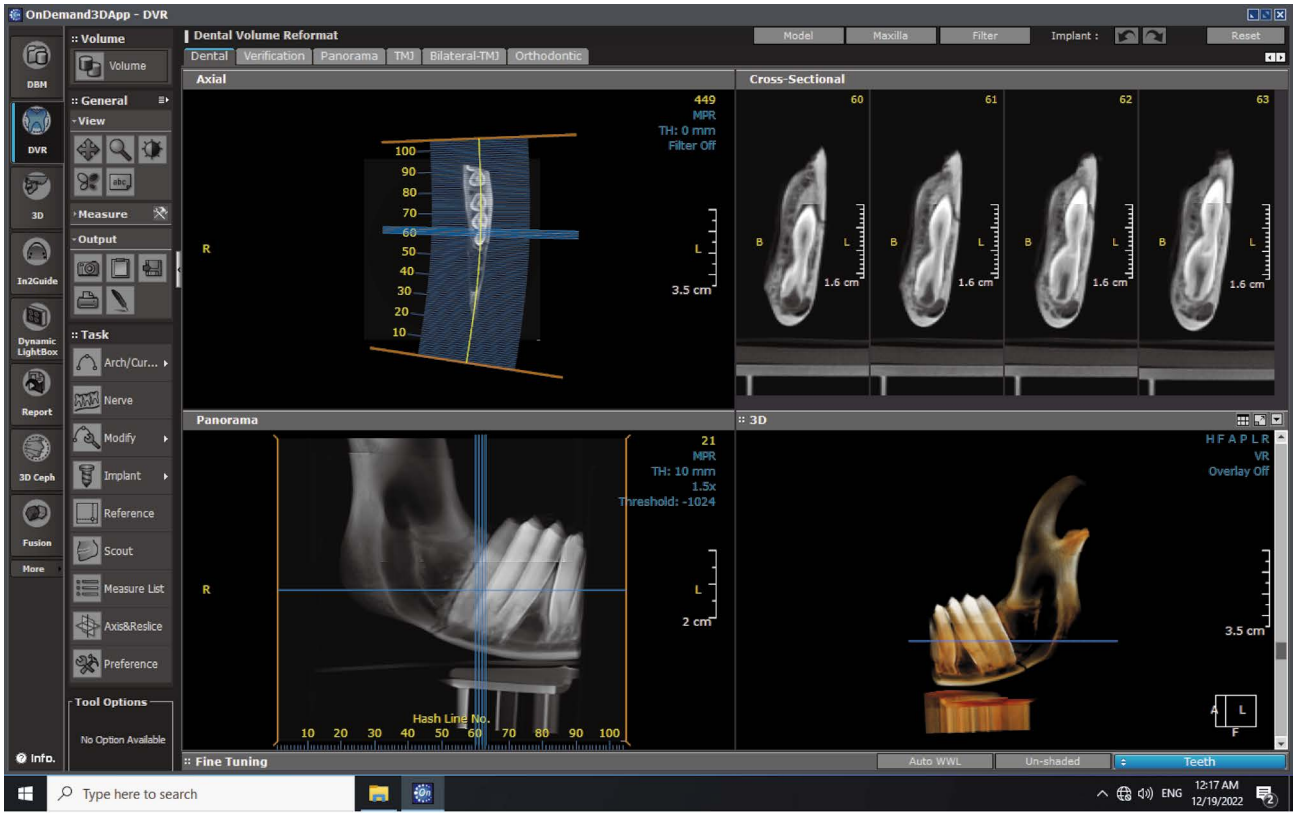

Fig. 3. Cross-sectional reconstruction images of non-stitched images of the ovine mandible with a 1 mm slice thickness and 1 mm slice interval.

Results

The inter-observer reliability was shown by a Fleiss kappa coefficient of 0.79 (range: 0.68-0.89; $P<0.05$), indicating good reliability according to Cohen's classification. The coefficient for intra-observer reliability was 1 for all 4 observers, indicating excellent intra-observer reliability.

Table 1 shows the diagnostic performance of the stitched and non-stitched images for the detection of non-displaced fractures of the ovine mandible. The sensitivity of the non-stitched and stitched images for detecting fracture lines was 90% and 85%, respectively, but the specificity of the non-stitched images was less than that of the stitched type. As shown in both image types, based on the calculated specificity and sensitivity, the AUCs of non-stitched (0.825) and stitched (0.862) images for detecting non-displaced fracture lines had a significant difference from an AUC of 0.50 ($P<0.05$) (Fig. 5). Although the AUC of the stitched images was slightly higher than that of the non-stitched images, the difference in diagnostic performance between the stitched and non-stitched images was not statistically significant ($P=0.747$).

Discussion

This study assessed the diagnostic performance of stitched and non-stitched cross-sectional CBCT images of non-displaced ovine mandibular fractures. In the present study, the AUC was found to be 0.825 for the non-stitched images, which was significantly different from an AUC of 0.50. Furthermore, the sensitivity and specificity of the non-stitched images for detecting non-displaced ovine fractures were 90% and 75%, respectively. These values were 85% and 87%, respectively, for stitched images. The present study's finding of higher specificity for the stitched images indicates fewer false positive diagnoses than with the non-stitched images. The AUC for the stitched images was 0.862, indicating higher diagnostic performance than for the non-stitched images, although this difference did not reach statistical significance. Thus, the present results showed an equivalent diagnostic performance of non-stitched and stitched CBCT images for detecting non-displaced ovine fractures.

Eskandarlou et al.[14] evaluated the detection of maxillofacial fractures by using a small and a large FOV and found that the small FOV had a higher diagnostic accuracy than

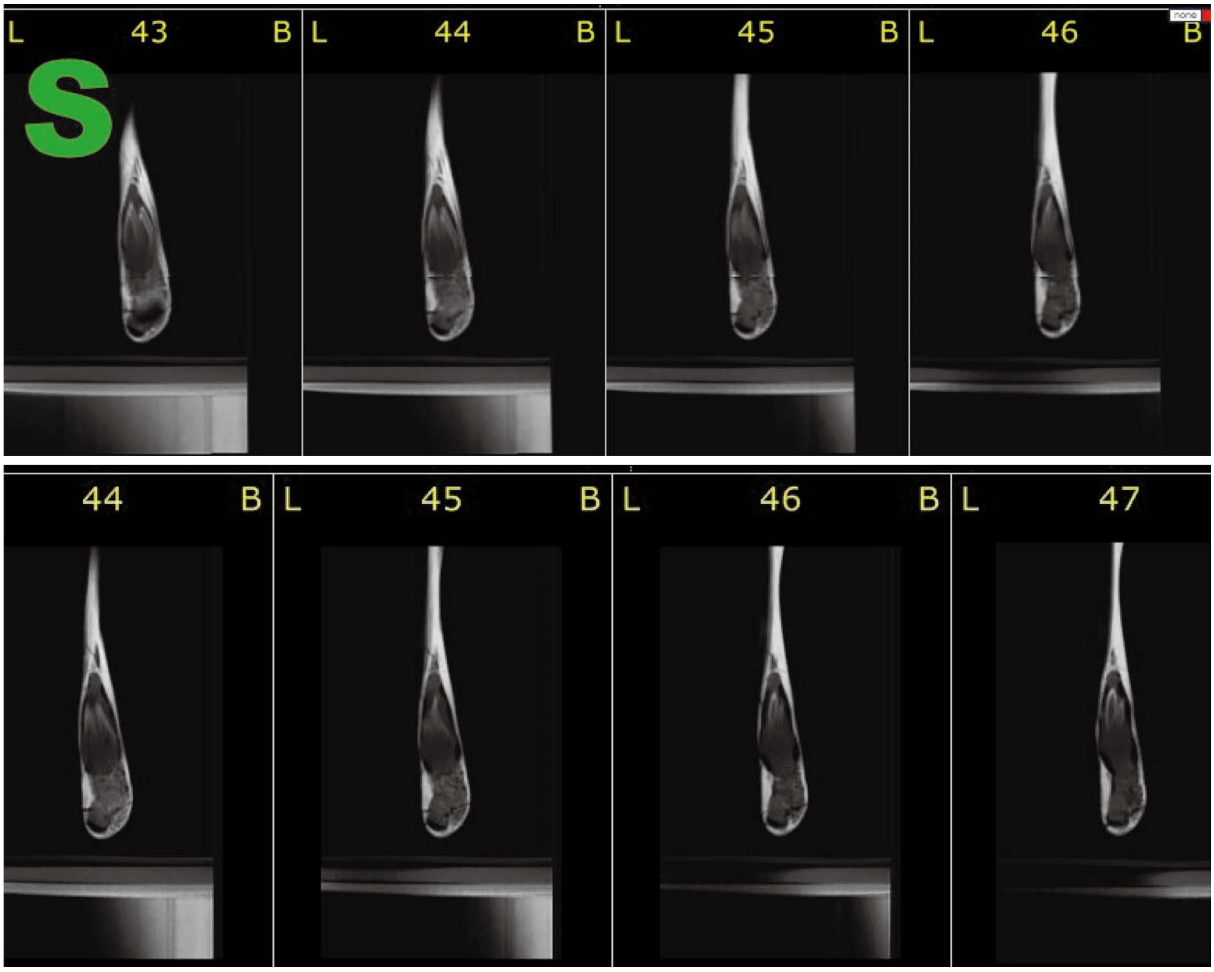

Fig. 4. Cross-sectional views of 2 similar areas of an ovine mandible with a fracture. A. Stitched image. B. Non-stitched image. A fracture line is observed in the lower third of the mandible.

Table 1. Diagnostic performance of non-stitched and stitched images for the detection of non-displaced fractures of the ovine mandible

Group	AUC	Standard error[a]	95% confidence interval[b]	*P* value	Sensitivity	Specificity
Non-stitched	0.825	0.089	0.94-0.63	<0.05	0.90	0.75
Stitched	0.862	0.075	0.96-0.68	<0.05	0.85	0.87

AUC: area under the receiver operating characteristic curve, a: DeLong et al.'s method, b: Binomial exact test

the large FOV. Many other studies have confirmed that a reduction in the size of FOV increases diagnostic accuracy.[17-21] In the present study, a small FOV (80×80 mm) was used for all scans to eliminate the effect of this confounder on the results.

A potential source of inherent artifacts exists in peripheral parts of volumetric CBCT scans due to the cone-beam geometry. In the present study, the ROI in the stitched images was not at the center of the image - instead, part of it was in the lower part of the FOV, and part of it was in the upper part of the FOV of the second scan, and the images overlapped. Nonetheless, no significant difference was found in diagnostic accuracy between the stitched and non-stitched images.

Hamed et al.[18] and Kim et al.[19] compared the diagnostic accuracy of linear measurements made on stitched images with direct measurements made on the samples. They reported no significant difference between the measurements, and the magnitude of the difference ranged from -0.25 to 0.5 mm (0.2% to 1.8%) in the study by Hamed et al.[18] Fur-

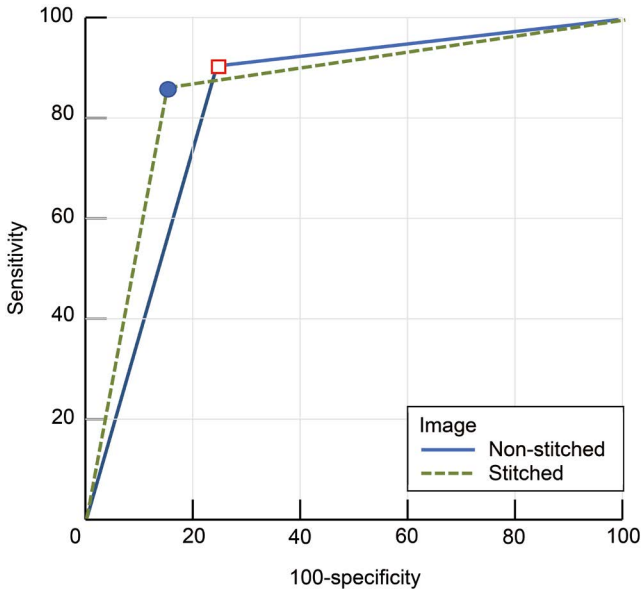

Fig. 5. Area under the receiver operating characteristic curve for stitched and non-stitched images, showing a slightly higher value for the stitched images.

thermore, Ozemre and Gulsahi[17] found a close correlation between the measurements made on stitched images and the actual values. They did not use any radiopaque marker for the measurable landmarks to prevent metal artifacts. Egbert et al.[6] used gutta-percha markers to identify anatomical points and found a significant difference between the 2 groups, which could have been due to the effect of radiopaque materials and metal artifacts on the diagnostic accuracy of the images. No metal restoration or marker was present in the present study conducted on ovine mandibles. Considering the usual presence of metal restorations in the oral cavity, further investigations are warranted in this regard.

The present study found good interobserver reliability (79%) among the 4 observers who evaluated the images. The intra-observer reliability was 1 for all 4 observers, indicating excellent intra-observer reliability. Wellenberg et al.[21] evaluated the geometric errors of stitched CBCT images of bone and reported the translation and rotation errors of the stitched images to be 3 mm and 3°, respectively, although the values were not statistically significant. They demonstrated that image noise, changing the object position during image acquisition, and stitching of different volumes of anatomical areas can affect the diagnostic accuracy of stitched images. A horizontal line appears at the site of stitching on stitched images, and the fracture lines were intentionally simulated in the same area; nonetheless, the presence of this horizontal line had no significant effect on the diagnostic accuracy of fracture detection. Wellenberg et al.[21] used an ovine cadaver; therefore, movement during image acquisition was not a problem in their study, similar to the present study.

Nonetheless, immobilization of trauma patients is a challenge in the clinical setting. Because non-displaced fractures are not visible on CBCT scans, the high diagnostic accuracy of stitched images can positively influence treatment planning, helping to detect the cause of pain and reassure patients.[20] Nonetheless, 2 main challenges remain in the use of stitched images - namely, immobilization of patients during the prolonged imaging period, particularly in trauma patients, and the effect of metal artifacts in the clinical setting. These issues warrant further clinical investigations on the effects of metal artifacts and the magnitude of motion artifacts on the diagnostic accuracy of stitched CBCT images.

In conclusion, no significant difference was found in the diagnostic performance of stitched and non-stitched cross-sectional CBCT images of non-displaced ovine mandibular fractures. Thus, considering the sufficiently high accuracy of stitched CBCT images, images from CBCT scanners with small FOVs may be reliably used after stitching if CBCT scanners with large FOVs are unavailable.

Conflicts of Interest: None

Acknowledgments

We would like to thank Dr. Mohammad Ebrahim Ghafari (Dental Sciences Research Center, Guilan University of Medical Sciences, Rasht, Iran) for his help in statistical analysis.

References

1. Schulze KW, Drage NA. Cone-beam computed tomography and its applications in dental and maxillofacial radiology. Clin Radiol 2020; 75: 647-57.
2. Scarfe WC, Farman AG, Sukovic P. Clinical applications of cone-beam computed tomography in dental practice. J Can Dent Assoc 2006; 72: 75-80.
3. Ahmad M, Jenny J, Downie M. Application of cone beam computed tomography in oral and maxillofacial surgery. Aust Dent J 2012; 57 Suppl 1: 82-94.
4. White SC. Cone-beam imaging in dentistry. Health Phys 2008; 95: 628-37.
5. Miracle AC, Mukherji SK. Cone beam CT of the head and neck, part 2: clinical applications. AJNR Am J Neuroradiol 2009; 30: 1285-92.
6. Egbert N, Cagna DR, Ahuja S, Wicks RA. Accuracy and reliability of stitched cone-beam computed tomography images. Imaging Sci Dent 2015; 45: 41-7.
7. Scarfe WC, Li Z, Aboelmaaty W, Scott SA, Farman AG. Maxillofacial cone beam computed tomography: essence, elements

and steps to interpretation. Aust Dent J 2012; 57 Suppl 1: 46-60.
8. Scarfe WC, Farman AG. What is cone-beam CT and how does it work? Dent Clin North Am 2008; 52: 707-30.
9. Kopp S, Ottl P. Dimensional stability in composite cone beam computed tomography. Dentomaxillofac Radiol 2010; 39: 512-6.
10. Nikbin A, Dalili Kajan Z, Taramsari M, Khosravifard N. Effect of object position in the field of view and application of a metal artifact reduction algorithm on the detection of vertical root fractures on cone-beam computed tomography scans: an in vitro study. Imaging Sci Dent 2018; 48: 245-54.
11. De Smet E, De Praeter G, Verstraete KL, Wouters K, De Beuckeleer L, Vanhoenacker FM. Direct comparison of conventional radiography and cone-beam CT in small bone and joint trauma. Skeletal Radiol 2015; 44: 1111-7.
12. Kaeppler G, Cornelius CP, Ehrenfeld M, Mast G. Diagnostic efficacy of cone-beam computed tomography for mandibular fractures. Oral Surg Oral Med Oral Pathol Oral Radiol 2013; 116: 98-104.
13. Miloro M, Ghali GE, Larsen PE, Waite PD. Peterson's principles of oral and maxillofacial surgery. 2nd ed. New Haven: PMPH USA; 2004. p. 410.
14. Eskandarlou A, Poorolajal J, Talaeipour AR, Talebi S, Talaeipour M. Comparison between cone beam computed tomography and multislice computed tomography in diagnostic accuracy of maxillofacial fractures in dried human skull: an in vitro study. Dent Traumatol 2014; 30: 162-8.
15. Shokri A, Eskandarloo A, Norouzi M, Poorolajal J, Majidi G, Aliyaly A. Diagnostic accuracy of cone-beam computed tomography scans with high- and low-resolution modes for the detection of root perforations. Imaging Sci Dent 2018; 48: 11-9.
16. DeLong ER, DeLong DM, Clarke-Pearson DL. Comparing the areas under two or more correlated receiver operating characteristic curves: a nonparametric approach. Biometrics 1988: 44: 837-45.
17. Ozemre MO, Gulsahi A. Comparison of the accuracy of full head cone beam CT images obtained using a large field of view and stitched images. Dentomaxillofac Radiol 2018; 47: 20170454.
18. Hamed DA, El Dawlatly MM, El Dessouky SH, Hamdy RM. Accuracy of linear measurements obtained from stitched cone beam computed tomography images versus direct skull measurements. F1000Res 2019; 8: 166.
19. Kim MK, Kang SH, Lee EH, Lee SH, Park W. Accuracy and validity of stitching sectional cone beam computed tomographic images. J Craniofac Surg 2012; 23: 1071-6.
20. Abd Alsamad AM. Accuracy of linear measurements in stitched cone beam computed tomographic images an in-vitro study. Egypt Dent J 2017; 63: 2435-40.
21. Wellenberg RH, Dobbe JG, Erkkilä J, Maas M, Streekstra GJ. Marker-less assessment of the geometric error of fused cone-beam computed tomography images of the foot constructed using stitching software. Acta Radiol 2021; 62: 1341-8.